MDPI

Article

Fluid-Structure Interaction of Flexible Whisker-Type Beams and Its Implications for Flow Sensing by Pair-Wise Correlation

Raphael Glick *, Muthukumar Muthuramalingam and Christoph Brücker

School of Mathematics, Computer Science and Engineering, University of London, London ECV1 0HB, UK; muthukumar.muthuramalingam@city.ac.uk (M.M.); christoph.bruecker@city.ac.uk (C.B.)
* Correspondence: raphael.glick@city.ac.uk

Abstract: (1) Background: Sensing of critical events or flow signatures in nature often presents itself as a coupled interaction between a fluid and arrays of slender flexible beams, such a wind-hairs or whiskers. It is hypothesized that important information is gained in highly noisy environments by the inter-correlation within the array. (2) Methods: The present study uses a model sea lion head with artificial whiskers in the form of slender beams (optical fibres), which are subjected to a mean flow with overlaid turbulent structures generated in the wake of a cylinder. Motion tracking of the array of fibres is used to analyse the correlation of the bending deformations of pairs of fibres. (3) Results: Cross-correlation of the bending signal from tandem pairs of whiskers proves that the detection of vortices and their passage along the animals head is possible even in noisy environments. The underlying pattern, during passage of a vortex core, is a jerk-like response of the whiskers, which can be found at later arrival-times in similar form in the downstream whisker's response. (4) Conclusions: Coherent vortical structures can be detected from cross-correlation of pairs of cantilever-beam like sensors even in highly turbulent flows. Such vortices carry important information within the environment, e.g., the underlying convection velocity. More importantly in nature, these vortices are characteristic elementary signals left by prey and predators. The present work can help to further develop flow, or critical event, sensory systems which can overcome high noise levels due to the proposed correlation principle.

Keywords: tandem cylinders; flexible beams; fluid–structure interaction; whisker sensing; cross-correlation; coherent vortices; convection velocity; optical fiber sensors; pinniped head

1. Introduction

Fluid–structure interactions of flexible cantilevered cylinders have been studied for a long time [1]. Most of the applications addressed in these studies were related to high-Reynolds-number flows in oil risers or heat converters, to name a few. Interest also arose in the flow around filamentous structures with sub-millimeter diameter, which are often found in nature in various forms. They function as antennae or sensing structures in animals such as in bats, cockroaches, or spiders [2]. Furthermore, they appear as whiskers in pinnipeds, or seals, that live in the aquatic environment. The typical Reynolds-number of flows around those whisker-type structures is in the range between 10 and 1000 with Re_d based on the characteristic diameter of the whisker diameter d. As a typical feature, these sensing elements do not appear as a single structure but are instead arranged in arrays. The signal output is expected to be largely influenced by the arrangement of sensory hairs, as investigated in Bruecker and Rist [3]. This may allow the distinction of complex patterns from their spatio-temporal signature. It seems probable that this is important in nature, where the multi-signal sensor output needs to be selective enough to trigger specific tasks such as flow control or escape behavior, under the influence of turbulent background noise. The first studies into neurological relevance of the cross-correlation of the signals of neighbouring sensory hairs in the aquatic world, have been investigated on the lateral

line system of fish [4]. The spike trains taken from the primary afferent nerve fibres of a pair of neuromasts along the fish's lateral line system were cross-correlated, and the results provided the gross velocity of the fluid around the body of the fish. Therefore, the natural turbulent fluctuations in the water already transport the necessary information to retrieve the locomotive or convection speed of external flow patterns. The correlation hypothesis was also proven to work in engineering applications by using a pair of micro-pillar wall-shear sensors in a turbulent boundary layer flow [4], where the same cross-correlation was applied to recover the convection speed of the external flow around the plate.

Further advancements in sensory applications were found in tandem pairs of cylinders mimicking sensory hairs, regarding their side-by-side arrangement [5]. It was shown that the first cylinder can act as a flow preconditioner, serving to either improve the streamwise sensory response of the second sensor, or to shield it from streamwise fluctuations, while crossflow fluctuations remain unaffected. This would allow the system to be effective in sensing strong transverse motion patterns. Other aquatic species with slender cylinder-like sensors are sea lions and other pinnipeds, which can track their prey by using their whiskers as hydrodynamic sensors [6]. Recent studies on fluid–structure interaction of artificial whiskers showed that the most important pattern of the dynamic response signal does not come from the flow fluctuations, but from the pressure distribution in a vortex that passes the whiskers [7]. The authors constructed a model sea-lion head, with optical fibres acting as whiskers, to better understand how the animal's whiskers responded to stimulation. By mimicking the wake of prey or predators, in the form of von Karman type vortex streets, they found that the whiskers moved with each passing vortex in a jerk like manner. A distinctive "stick-slip" response pattern developed as a response to the pressure gradient in the vortex core [7]. This study showed, for the first time, that long whisker-type hairs are able to detect the passage of vortices, and that therefore, these sensors can be understood as "vortex detectors". This was a paradigm shift in the understanding of the whisker's response. Previous behavioral studies in controlled environments have shown that Harbor seals can sense the wake of prey over 30 s after the prey has past [8]. Our hypothesis is that weak signals like these can be better detected from a pair of neighbouring whiskers using their cross correlation, than from the bending signal of a single whisker alone. This could allow pinnipeds to distinguish a coherent signal from noise. Estebanez, Boustani and Destexhe [9] studied the neural response of rats to correlated whisker stimulation. They demonstrated that very few neurons responded to simple stimulation of a single whisker, but the neural response was far greater when correlated stimuli were introduced across multiple whiskers.

The goal of this study is to demonstrate that the pair-wise correlation of the whiskers' response can be used to detect coherent flow structures (vortices) passing the whiskers even in highly turbulent conditions, or at a very weak signal-to-noise ratio. This information is important firstly to detect typical vortex patterns left in the wake of prey or predators, and secondly to determine their velocity and convection direction relative to the swimming body. This could be an additional step forward in understanding the potential of such processing methods for target tracking. Our previous study, as a first step into using neural networks and deep learning [10], neglected the temporal pattern of the fluctuations and their coherence over the array of the fibres. Instead it used only the RMS values of the fluctuation amplitudes as input from all the different fibres. Nevertheless, this trained model is already able to predict the near-by upstream locations of the cylinder to within 1 cm accuracy [10]. The present study is a continuation of our previous work towards a more sophisticated model, which will also include the temporal information of the sensors. CFD simulations and experimental studies of the flow around a model of a seal head, are combined to determine the response of arrays of whiskers to turbulent incoming flow. The disturbance in the flow is produced by a cylinder upstream of the seal, which generated a von Karman vortex street. The vortices passing the whiskers generated fluctuating bending motions, which were recorded simultaneously for all whiskers and processed using cross-

correlation algorithms. Finally, gross flow velocity is estimated from those correlations and compared to the predictions from CFD.

2. Materials and Methods

2.1. Sea Lion Model with Whiskers

The experimental model is the same as described in our previous work [7] and the key features are described herein again. We use a 1:1 scaled model of the head of a sea lion with artificial whiskers (optical fibres, diameter $d = 0.75$ mm), with a similar length scale, and at similar positions to the biological example. In addition, the material of the fibres has an elastic modulus, and diameter, similar to the natural whiskers [7]. The array of optical fibers are inserted through holes from the backside of the 3D printed model and are illuminated from one end such that the tips of the free fibre ends appear as bright spots, on both sides of the head. The fibres therefore represent one-sided clamped flexible cantilever beams with circular cross-section, interacting with the flow.

2.2. Experimental Setup for Motion Tracking

The experimental setup is the same as described in our previous work [7], except for the differences in experimental procedure and data processing. The sea lion model with its artificial whiskers, is mounted inside the measurement chamber of a return type open surface water tunnel with a velocity range of 0.1 to 2 m/s. Flow straighteners were installed in the settling chamber, situated before the convergent section, to achieve uniform flow in the test section. The test section is 40 cm wide × 50 cm depth × 120 cm in length and transparent on all sides to provide optical access for flow studies. The model was placed at the centre of the test section, 70 cm down stream from the inlet as shown in Figure 1, and a wake generating cylinder was placed upstream of the sea lion model to generate turbulent vortical flow features that would pass the head and whiskers. The experiments were conducted with a cylinder of diameter $D = 30$ mm at three flow velocities U_∞ of 20, 25 and 30 cm/s. These parameters were selected based on findings by Miersch et al. [11]. A high-speed camera (ProcImage 500-Eagle, Photon Lines LTD, Banbury, UK) at a sampling rate of 250 Hz was used to track the motion of the whiskers on one side of the sea lion model, as shown in Figure 1b. It had a pixel size of 1280 × 1024 which relates to a physical dimension of 238 × 190 mm. The built-in function in the camera calculates the tip coordinates in the (x, y) coordinate system of each light spot automatically using the barycentre mode. The measured signals are the tip deflections of each of the optical fibers captured simultaneously, which is directly proportional to the applied bending moment at the shaft of the whiskers (Euler–Bernoulli beam theory). For further details see [7,10].

2.3. Flow Studies Using PIV and CFD

A combined experimental and numerical study using Particle image velocimetry (PIV) and CFD was done to characterize the flow conditions in front and around the sea lion head. For PIV, a 2 mm thick laser light sheet was focused on the region upstream of the snout region of the sea lion head. The PIV images had a pixel size of 1280 × 800 with a physical dimension of 152 × 95 mm. Neutrally buoyant particles of 50 microns were seeded in the water tunnel, and were recirculated within the tunnel until the right amount of particles required for the PIV were observed. The images were captured with a Phantom Miro M310 camera (Phantom Ametek, Wayne, NJ, USA), using a 45 degree slant mirror as shown in Figure 1a at a frame rate of 250 Hz and for a flow time of 4 s. Classical digital cross-correlation (DPIV) is used to obtain the 2D velocity vector field in the plane, using an iterative interrogation window (IW) refinement procedure (starting from 64 × 64 IW size) and sub-pixel accuracy analysis from a Gaussian fit to the correlation peak.
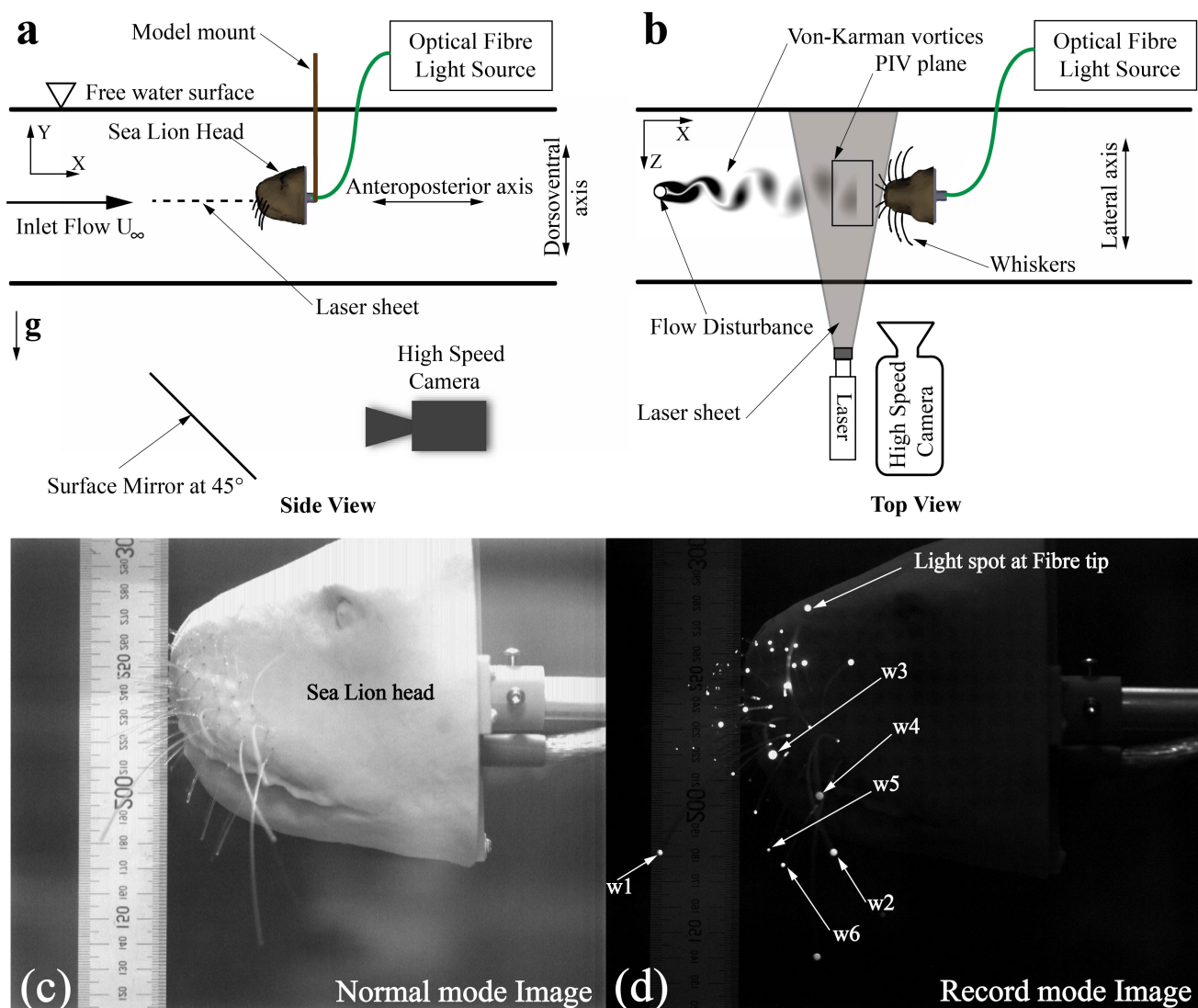
Figure 1. Schematic diagram of the experimental set-up, modified after [7]. (**a**) Side-view (**b**) Top-view. Von-Karman vortex street is shown for representation. (**c**) Normal mode photograph of the model from the camera (Scale in mm). (**d**) Image from the camera with reduced light and fibre optic light switched ON (the tips of fibres are visible as light spot) Note that the whisker numbering is used in the discussion of results.

Figure 2 shows the computational domain used in LES simulations. The domain extends 400 mm in *Y* and *Z* directions and 1200 mm in *X* direction, which is comparable to the experiments. The outer faces are discretised with 2 mm structured hexahedral elements and the cylinder circumference is discretised with 400 mesh points. The first cell distance from the cylinder surface was 0.04 mm which resulted in a y+ value less than 1. The domain around the sea lion head was meshed with unstructured tetrahedral elements which resulted in a total mesh size of 9.2 million. The Large Eddy Simulation was performed with commercial CFD solver: Ansys Fluent, (Ansys, version 19.0, Canonsburg, PA, USA) using WALE (Wall-Adapting Local Eddy-viscosity) subgrid scale model [12].

In a first approximation, no whiskers were considered in the mesh, as the key information on the FSI necessary for testing the correlation hypothesis has already been obtained in high quality from prior detailed experiments [7]. The complementary CFD simulations are mainly utilised to determine the global flow field around the head, which is difficult to achieve otherwise. It is difficult to determine from a PIV experiment because of the whiskers obstructing the optical view in the light-sheet plane close to the surface of the model. Furthermore, a fully two-way coupled FSI simulation of the current 3D problem

requires an immense amount of computing effort; it would require solving the FSI at all required spatial and temporal scales, whilst fully resolving the dynamics of all whiskers along the model seal head. As the diameter of the whiskers is more than two orders of magnitude smaller than the characteristic scale of the head, very small time-steps on a very large mesh need to be considered for physical time periods of minutes. This illustrates the dilemma of such simulations and explains our approach of combining CFD (without the whiskers) and experimental data (with whiskers) with exactly the same boundary conditions. Note that we assume in this first approximation that the gross flow around the head is not affected by the presence of the tiny whiskers. The inlet was specified with constant velocity of 30 cm/s with inlet turbulence value of 0.3%. The momentum equations are discretised with central differencing and second order scheme was used in time discretisation with a time step value of 0.004 s which relates to 120 time steps per shedding cycle calculated from the Strouhal frequency.
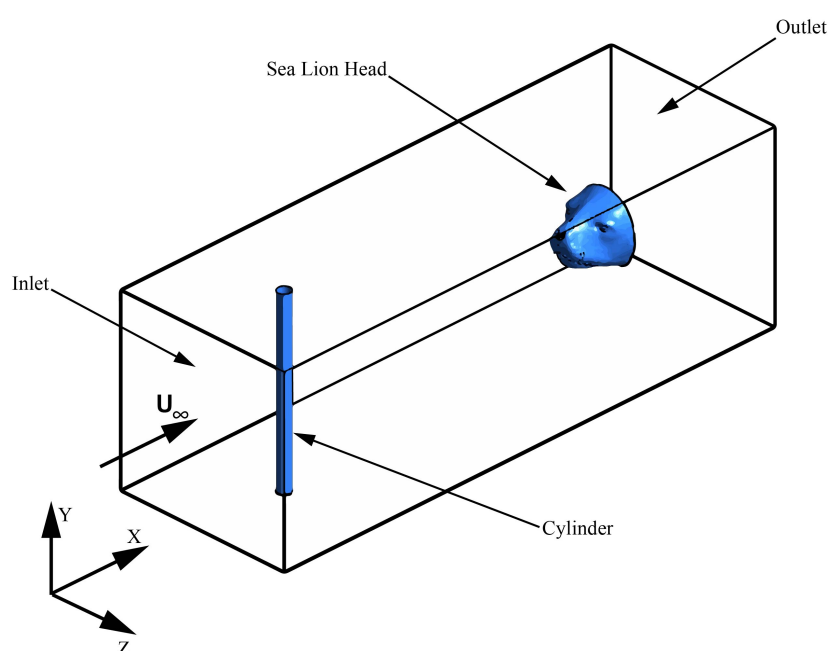

Figure 2. Sketch of the CFD domain and the flow configuration similar to the experiment. The domain extends 0.4 m in *Y* and *Z* directions and 1.2 m in *X* direction.

3. Results

Figure 3 shows an instantaneous flow pattern of the cylinder wake when the cylinder is placed ahead of the snout of the model along the body axis. The underlying disturbances in the flow field are produced by the von Karman vortex street, generated in the wake of the upstream cylinder, producing a periodic shedding of coherent vortices (quasi 2D vortex rollers, with their axes aligned with the cylinder axis). The Reynolds-number, defined with the free-stream velocity and the diameter *D* of the cylinder, is $Re_{cyl} = 9000$, which is clearly in the turbulent wake regime. The shedding pattern in the horizontal plane (crossing the model axis) is similar to that of the so-called "inverse" von Karman vortex street, which is found in the wake of swimming fish due to the periodic body and fin undulation [13]. The direction of rotation of the vortices in the fish wake is the inverse of that which is found in the cylinder wake, however the pressure distribution in the vortices is similar [14]. For comparison, Figure 3 also illustrates the time-averaged flow pattern. From that we see the typical velocity deficit in the wake of the cylinder and the "bow wake" effect in front of the snout (due to the effect of the displacement body). As a consequence, short whiskers around the front part of the snout "feel" the flow disturbances passing by with lower velocity than long whiskers at the more lateral side of the snout, which stand out of the bow wake region in the free stream.
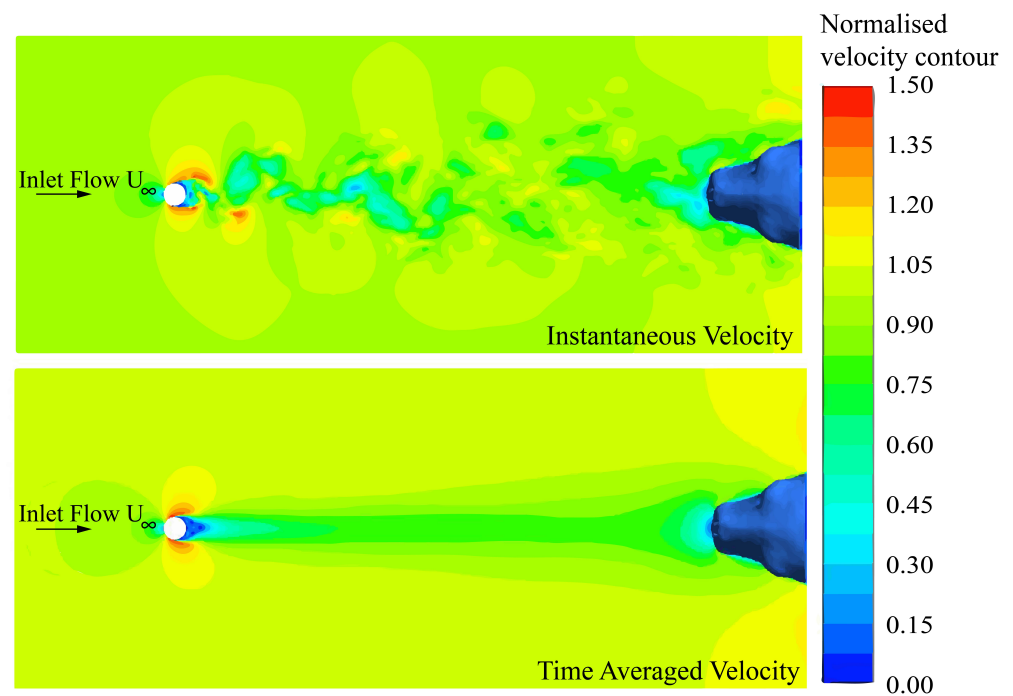
Figure 3. Velocity field through the test section from CFD Simulation (displayed as color-coded contours of constant streamwise velocity). Top: Instantaneous velocity field, Bottom: Time-averaged flow pattern.

The velocity field results from LES were compared against the PIV measurements in the region upstream of the snout, both show a similar decrease of the streamwise velocity near the snout, see Figure 4. Note, that the bow-wake effect has been shown to play a large role in hunting and predator escape as documented in Kogan et al. [15].
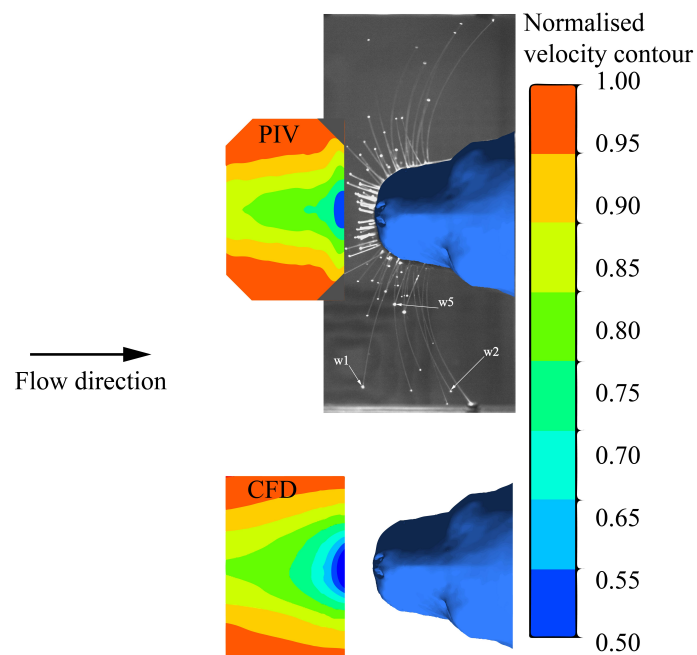

Figure 4. Bow-wake region in front of the snout from experimental flow field measurement using PIV compared to the CFD flow field (displayed as color-coded contours of constant streamwise velocity).

3.1. Typical Whisker Response

In the following sections, the results are presented for both short and longer whiskers (50 mm and 100 mm, respectively), the short ones being tested with the cylinder placed along the body axis, while for the long ones the cylinder was moved transversely to a distance of 100 mm away from the axis. This is to ensure that the vortices pass along the tips of the whiskers in all experiments. Note that the major component of the bending motion is in streamwise direction, parallel to the dominant fluctuations in the velocity field of the shed vortex rollers. We have taken a 3–4 min recording for each of the inlet velocities U_{inf} = 20, 25, and 30 cm/s . Our analysis data set size is typically a time-window of around 40 s, therefore for each experiment we have 5–6 independent samples. An example of a short sequence of individual whisker responses to the passing of von Karman vortices is given in Figure 5, shown for whiskers w1 and w2 with a freestream velocity U_{inf} at 25 and 30 cm/s. The plot shows the time-dependent tip location of the bending beams (in streamwise direction) with the mean removed. With a typical Strouhal number of roughly 0.2 for cylinder wake flows [16] we expect the shedding frequency at 30 cm/s to be 2 Hz (for cylinder diameter of D = 30 mm), which should correlate with the periodicity of the whisker's motion. As can be seen in Figure 5 the tip motion of whisker w1 exemplifies the expected periodic character of the deflections, overlaid with random fluctuations due to the turbulent nature of the flow. For comparison, the tip-motion of whisker w2 is overlaid on the same plot, which is positioned in the roughly the same horizontal plane further downstream of whisker w1 and has the same length as w1. It is obvious from the time-patterns that the response is similar, albeit shifted in time. This calls for the investigation of the pair-wise correlation hypothesis given above.
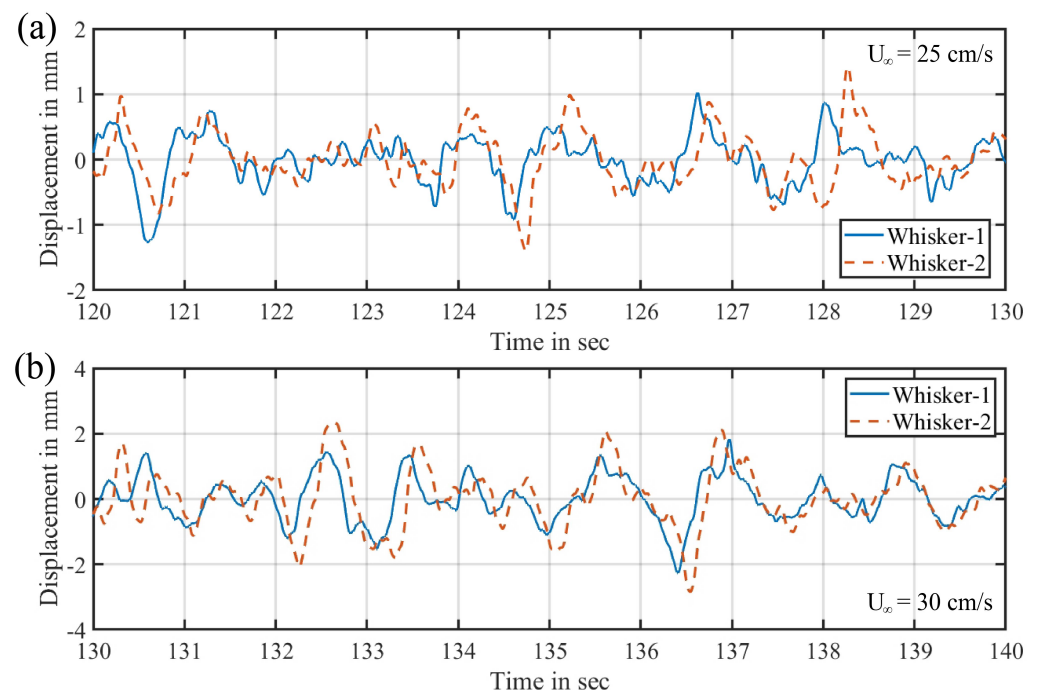

Figure 5. Fluctuating tip-motion of a pair of whiskers w1 and w2 in the wake of the cylinder (**a**): freestream velocity U_∞ = 25 cm/s, (**b**): freestream velocity U_∞ = 30 cm/s. The time-traces show a series of similar characteristic jerk motions, off-set from each other by the time taken for vortices to travel the distance between the whiskers (mean component subtracted).

3.2. Pair-Wise Correlation of Whisker Motion

The characteristic jerk-type response of the whiskers during passage of a vortex is the signal that provides the largest contribution to the correlation peak, while random motion does not correlate. To test this hypothesis, the temporal traces of the whiskers' tip-motion were cross-correlated (time-window of 40 s) and the time-lag at the peak location was

considered to represent the corresponding average travel time of the vortices between the tip-locations. The estimated convection velocity values between the pair of whiskers w1 and w2 are given in Table 1, in addition to the free stream velocity, and the local velocity at the location of whisker w2, taken from the LES results of the flow field around the head. As both whisker w1 and w2 are long enough to extend outside the influence of the bow wake of the model (w1 and w2 as shown in Figure 1, both of length 100 mm), the estimated convection velocities are close to the free-stream velocity. A slight overestimation is observed due to the body displacement effect, shown in Figure 3 by the accelerated flow around the sides of the head, where the whiskers w1 and w2 are located. The reference velocities shown in Tables 1 and 2 are taken from the LES results at the whisker w2 location.

Table 1. Results of the measured convection velocity by cross correlation (CC) of whiskers w1 and w2, situated outside of the influence of the bow wake. Local reference velocity at position w2 is taken from the LES simulations in Figure 3.

Freestream Velocity U_∞ (cm/s)	Local Velocity (cm/s)	CC Velocity (cm/s)
20	20.8	21.2
25	26.0	26.1
30	31.2	30.9

Table 2. Results of the measured convection velocity by CC of whiskers w1 and w5, the latter being situated inside of the influence of the bow wake. Local reference velocity at location w5 is taken from the LES simulations in Figure 3.

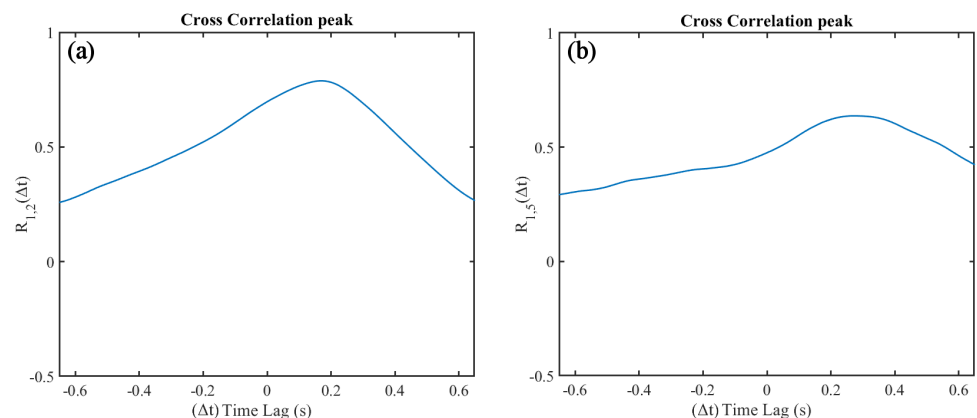| Freestream Velocity U_∞ (cm/s)	Local Velocity (cm/s)	CC Velocity (cm/s)
20	18.2	18.0
25	22.8	22.6
30	27.3	26.9

Figure 6. Typical profiles of the cross-correlation function around the peak for tunnel flow speed at 20 cm/s. (**a**) CC of whiskers w1 and w2, peak value of 0.78. (**b**) CC of whiskers w1 and w5, peak value of 0.62. The greater time delay in B) is due to the lower velocity, as discussed above.

Another pair of whiskers were chosen for further testing the correlation hypothesis, see Figure 6. This time, a pair with different lengths were selected (w1 and w5, the latter with 50 mm half the length of w1). This was to investigate possible effects of structural instabilities of the whiskers on the CC results, as different beam lengths also means different characteristic frequencies of the bending modes under dynamic fluid loads. The calculated free stream velocity values from this pair-wise correlation in Table 2 are notably lower than the actual free stream velocities since much of whisker w5's length is inside the bow wake region. Therefore the vortices are travelling at lower convection speeds across w5. This

is also justified by the lower velocity reference values at the whisker tip location, from the LES.

All correlations so far were done with a time-window of 40 s, which is equivalent to the passage of about 80 shed vortices. Typical SNR values of the CC peak (ratio of the primary peak height to 2nd peak) were found to be 10 for all tested configurations. For steady background flows, even a shorter time window containing a jerk-signal of a single vortex may be strong enough for a reliable cross correlation. However, the turbulent nature of the wake flow at Re_{cyl} = 9000 herein requires a larger number of coherent structures passing by to keep such a high SNR of the CC peak. When the time window was shortened below 10 s, the quality of the CC peak diminished and random fluctuations caused shallow, split CC peaks, which could not be qualified as representative of the overall flow field. On the other hand, when the time window became too large, the CC peak became flattened due to the overall time-averaging effect of the turbulent flow. The above discussion pertaining to the influence of the number of events on the CC, only relates to a single whisker pair. It it obvious that a larger number of whiskers, given that there are typically 38 whiskers on each side of the sea lion, would greatly improve the SNR when using a global correlation. Seals may also detect single vortex structures in a turbulent environment by using a global correlation involving all their whiskers simultaneously.

3.3. Simulation of Noise Effects

For further investigation of the influence of background noise on the correlation signal we use the theoretically derived response of the beam for the passing of a vortex (see the mathematical derivation given in Appendix 1 in [7]). The Gaussian pressure drop in the core of the vortex leads to a jerk-type response of the beam in form of the time-derivative of the Gaussian:

$$J(t) \propto \Gamma \frac{(U_\infty t - x_0)}{R} exp\left(\frac{-2(U_\infty t - x_0)^2}{R^2} \right) \tag{1}$$

where Γ is the circulation strength of the vortex, R is the radius of the vortex core and x_0 is the location of the leading whisker relative to the trailing whisker (position $x = 0$). At $t = 0$ the incoming vortex has hit w1 at $x = -x_0$ and travels further towards w2, where it hits with a time-lag of $\Delta t = x_0/U_\infty$, i.e., the time taken for the vortex to travel the distance between both whisker. This signal is used to investigate the cross-correlation with different levels of noise overlaid. Figure 7a, shows a generated jerk signal, with high levels of random background noise and its time-shifted counterpart, again with high level of noise. Despite this, without any filtering or smoothing, a strong correlation can still be seen in the expected region of time lag as shown in Figure 7b. However, the maximum position of the curve is not clearly visible as it was in the previous situation without noise. The random noise introduces uncertainty in the position of the true peak. As the base signal is of type of a Gaussian function, the peak region in the cross correlation profile can be approximated with a Gaussian function, too. This technique is known in Digital Particle Image Velocimetry as peak fitting and allows one to achieve sub-pixel resolution [17]. The same methodology it is used herein to fit the peak region, see Figure 7c. As a result, we have found that even for high noise levels, where the random noise is almost 50% of the amplitude of the signal, the fitted Gaussian curve produced the time lag with 95% confidence, to within ±5.4% of the correct time lag.
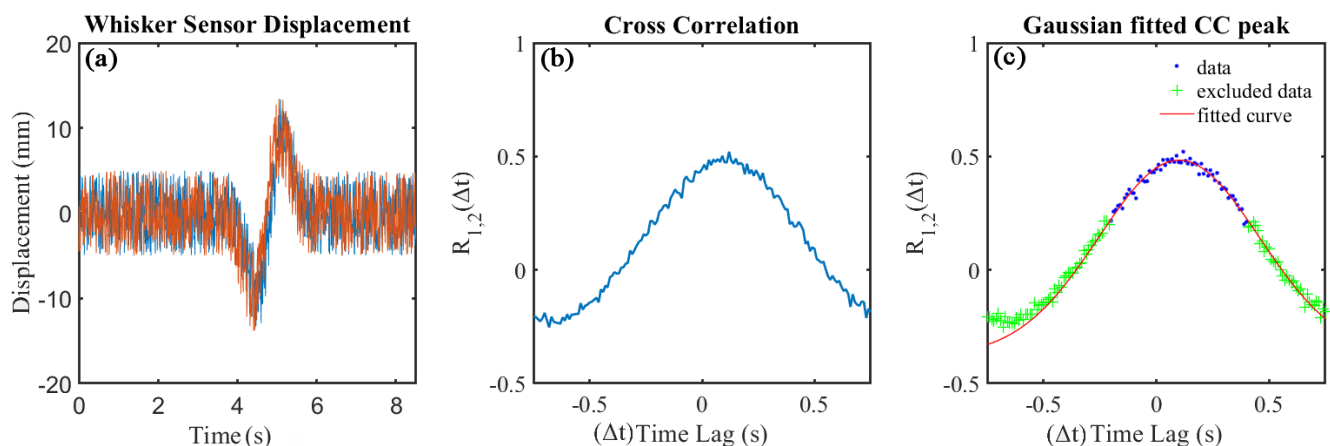
Figure 7. Synthetic jerk-pulse with added random noise and its CC profile. (**a**) jerk signal with an SNR of 2.6 in original (red) and time-shifted with 0.1 s (blue), noise addition is random and independent in both signals. (**b**) CC of the noisy signals, showing erratic fluctuations near the peak. (**c**) Gaussian curve fit in the peak region with a clear maximum at the expected time-lag.

4. Discussion

Previous work by one of the authors and colleagues [4] describes the lateral line system of fish, and how this system can determine gross flow direction and velocity from cross-correlation of the signals from the neighbouring neuromasts. The present study aimed to test this hypothesis for application in whisker-type sensors.

The pair-wise correlation of flexible beam motion for sensory application in nature (and engineering), has been investigated herein for slender cantilever beams of sub-millimeter diameter, similar in shape, size and mechanical properties to those of sea lion whiskers (for detailed material parameters see our previous work [7]). For such whiskers, paired with typical animal swimming speeds of order of 1 m/s, the Reynolds-number of the local flow around the beam is still in the low to moderate Reynolds-number regime ($Re_d < 1000$). When tested for their response to a von Karman vortex street of an upstream located cylinder we found that each time a coherent vortex passes a beam, a jerk-type response of the beam is observed, which is caused by the force induced by the Gaussian pressure drop in the core of the vortex (see also the mathematical derivation given in the Appendix 1 in [7]). This signal is an ideal candidate for estimating the convection velocity of these embedded structures via a pair-wise correlation of the bending of neighbouring beams. Indeed, the correlation signals show a high signal-to-noise ratio of about 10 (ratio between 1st and 2nd peak) and can clearly decode the convection velocity, in low-turbulence background flows even from a single vortex event. On the other hand, the strong correlation also provides a way to distinguish existing vortical structures from noise when such events hit the whiskers along the body of the animal. This allows the animal to sense characteristic hydrodynamic signals left by prey or predators in their wake. Additionally, this could also allow for further investigation into whether the sea lion, or other pinnipeds, utilise the combined signals from multiple whiskers, and if the time shift of hydrodynamic stimuli is a factor.

Engineering applications of pairs or arrays of whisker-type sensors can be envisioned in a similar way to detect hydrodynamic signals of wake-generating bodies or swimmers in aquatic environments, or to provide a robust way of sensing the swimming speed. On a smaller scale, flexible beams in the form of micro-pillars have already been used for measurements of the wall-shear stress signals in turbulent boundary layer flows in air and water [18]. Therein, the passage of strong events of sweeps or ejections could be detected in a similar way from cross-correlation as a kind of "event" detector. Further improvement of the accuracy of the time-lag is possible using a Gaussian fitting procedure of the correlation-peak. The beauty of such signal processing is that such events can be

detected even under conditions of high-levels of noise (weak SNR). In addition, it does not require detailed calibration of the single sensors, it is only necessary to have a priori knowledge of their dynamic response, see also [19]. Therefore, such data processing is superior to any processing of a single sensor.

The investigations herein are limited to thin slender beams with typical inter-spacing of more than 20 times the diameter *d* of the whiskers, similar to the widely distributed whiskers of the seal. These are therefore only minimally affected by galloping, which is often observed in tandem arrangements of larger cylinders [1]. In addition, we have only tested the pair-wise correlation for whisker pairs placed in a similar horizontal plane of the head. Certainly, the more complex arrangement of the whiskers on a pinnipeds' head requires further study of these effects and possible applications to 3D flow disturbances. Future research will focus on furthering the usage of the correlation hypothesis for the detection of distance and direction of the source. In principle, the disturbances generated by the cylinder are periodic patterns, however our theoretical results with single jerk-signals show that the pair-wise correlation can also work based on single pulses or events, where single vortices hit the head. This is current work in our lab, which may also support behavioral studies on seals to detect the direction of incoming hydrodynamic disturbances [20].

Abbreviations

The following abbreviations are used in this manuscript:

CC	Cross Correlation
CFD	Computational Fluid Mechanics
DPIV	Digital Particle Image Velocimetry
FSI	Fluid Structure Interaction
IW	Interrogation Window
LES	Large Eddy Simulation
SNR	signal to Noise Ratio
PIV	Particle Image velocimetry
Re_{cyl}	Re-number based on cylinder diameter
Re_d	Re-number based on whisker diameter
RMS	Root Mean Square

References

1. Bearman, P. Vortex shedding from oscillating bluff bodies. *Ann. Rev. Fluid Mech.* **1984**, *16*, 195–222. [CrossRef]
2. Barth, F.; Humphrey, J.; Secomb, T. *Sensors and Sensing in Biology and Engineering*, 1st ed.; Springer: New York, NY, USA, 2003.
3. Brücker, C.; Rist, U. *Complex Flow Detection by Fast Processing of Sensory Hair Arrays*; Springer: Berlin/Heidelberg, Germany, 2014.
4. Chagnaud, B.; Brücker, C.; Hofmann, M.; Bleckmann, H. Measuring Flow Velocity and Flow Direction by Spatial and Temporal Analysis of Flow Fluctuations. *J. Neurosci.* **2008**, *28*, 4479–4487. [CrossRef] [PubMed]
5. Axtmann, G.; Hegner, F.; Brücker, C.; Rist, U. Investigation and prediction of the bending of single and tandem pillars in a laminar cross flow. *J. Fluids Struct.* **2016**, *66*, 110–126 [CrossRef]
6. Dehnhardt, G.; Mauck, B.; Bleckmann, H. Seal whiskers detect water movements. *Nature* **1998**, *394*, 235–236. [CrossRef]
7. Muthuramalingam, M.; Brücker, C. Seal and Sea lion Whiskers Detect Slips of Vortices Similar as Rats Sense Textures. *Sci. Rep.* **2019**, *9*, 12808. [CrossRef] [PubMed]
8. Wieskotten, S.; Dehnhardt, G.; Mauck, B.; Miersch, L.; Hanke, W. Hydrodynamic determination of the moving direction of an artificial fin by a harbour seal (P*hoca vitulina*). *J. Exp. Biol.* **2010**, *293*, 2194–2200 [CrossRef] [PubMed]
9. Estebanez, L.; El Boustani, S.; Destexhe, A. Correlated input reveals coexisting coding schemes in a sensory cortex. *Nat. Neurosci.* **2012**, *15*, 1691–1699 [CrossRef] [PubMed]
10. Elshalakani, M.; Muthuramalingam, M.; Brücker, C. A deep-learning model for underwater position sensing of a wake's source using artificial seal whiskers. *Sensors* **2020**, *20*, 3522. [CrossRef] [PubMed]
11. Miersch, L.; Hanke, W.; Wieskotten, S.; Hanke, F.; Oeffner, J.; Leder, A.; Brede, M.; Witte, M.; Dehnhardt, G. Flow sensing by pinniped whiskers. *Philos. Trans. R. Soc. B Biol. Sci.* **2011**, *366*, 3077–3084 [CrossRef] [PubMed]
12. ANSYS. *Ansys Fluent Tutorial Guide*; ANSYS: Houston, TX, USA, 2019.
13. Müller, U.; Van Den Heuvel, B.; Stamhuis, E.; Videler, J. Fish foot prints: Morphology and Energetics of the wake behind a continuously swimming mullet (Chelon Labrosus Risso). *J. Exp. Biol.* **1997**, *200*, 2893–2906.
14. Videler, J.; Muller, U.; Stamhuis, E. Aquatic vertebrate locomotion: Wakes from body waves. *J. Exp. Biol.* **1999**, *202*, 3423–3430. [PubMed]
15. Kogan, I.; Pacholak, S.; Licht, M.; Schneider, J.W.; Brücker, C.; Brandt, S. The invisible fish: Hydrodynamic constraints for predator-prey interaction in fossil fish Saurichthys compared to recent actinopterygians. *Biol. Open* **2015**, *4*, 1715–1726. [CrossRef] [PubMed]
16. Blevins, R. *Flow-Induced Vibration*, 2nd ed.; Van Nostrand Reinhold Company: New York, NY, USA, 1990.
17. Raffel, M.; Willert, C.; Scarano, F.; Kähler, C.; Wereley, S.; Kompenhans, J. *Particle Image Velocimetry: A Practical Guide*, 2nd ed.; Springer: Berlin/Heidelberg, Germany, 2007.
18. Brücker, C.; Spatz, J.; Schroder, W. Feasability study of wall shear stress imaging using microstructured surfaces with flexible micropillars. *Exp. Fluids* **2005**, *39*, 464–474
19. Brücker, C.; Bauer, D.; Chaves, H. Dynamic response of micro-pillar sensors measuring fluctuating wall-shear-stress. *Exp. Fluids* **2007**, *42*, 737–749
20. Krüger, Y.; Hanke, W.; Miersch, L. Detection and direction discrimination of single vortex rings by harbour seals (*Phoca vitulina*). *J. Exp. Biol.* **2018**, *221*. [CrossRef] [PubMed]